Modelling the transport of carbonic acid anions through anion-exchange membranes

ARTICLE *in* ELECTROCHIMICA ACTA · OCTOBER 2003

Impact Factor: 4.5 · DOI: 10.1016/S0013-4686(03)00485-7

4 AUTHORS:

Victor Nikonenko
Kuban State University
93 PUBLICATIONS **1,768** CITATIONS
SEE PROFILE

Konstantin Andreevich Lebedev
Kuban State University
20 PUBLICATIONS **164** CITATIONS
SEE PROFILE

José A. Manzanares
University of Valencia
117 PUBLICATIONS **2,047** CITATIONS
SEE PROFILE

Gerald Pourcelly
Université de Montpellier
169 PUBLICATIONS **3,089** CITATIONS
SEE PROFILE

Available online at www.sciencedirect.com
SCIENCE DIRECT®
PERGAMON
Electrochimica Acta 48 (2003) 3639–3650
ELECTROCHIMICA Acta
www.elsevier.com/locate/electacta

Modelling the transport of carbonic acid anions through anion-exchange membranes

V. Nikonenko [a,1], K. Lebedev [a,1], J.A. Manzanares [b,2], G. Pourcelly [c,*]

[a] *Department of Physical Chemistry, Kuban State University, 149 Stavropolskaya str., Krasnodar 350040, Russia*
[b] *Department of Thermodynamics, University of Valencia, Valencia, Spain*
[c] *Institut Européen des Membranes, Université Montpellier II, UMR 5635, CC 047, Place Eugène Bataillon, 34095 Montpellier cédex 5, France*

Received 25 March 2003; received in revised form 9 June 2003; accepted 16 June 2003

Abstract

Electrodiffusion of carbonate and bicarbonate anions through anion-exchange membranes (AEM) is described on the basis of the Nernst–Planck equations taking into account coupled hydrolysis reactions in the external diffusion boundary layers (DBLs) and internal pore solution. The model supposes local electroneutrality as well as chemical and thermodynamic equilibrium. The transport is considered in three layers being an anion exchange membrane and two adjoining diffusion layers. A mechanism of competitive transport of HCO_3^- and CO_3^{2-} anions through the membrane which takes into account Donnan exclusion of H^+ ions is proposed. It is predicted that the pH of the depleting solution decreases and that of the concentrating solution increases during electrodialysis (ED). Eventual deviations from local electroneutrality and local chemical equilibrium are discussed.

Keywords: Anion-exchange membranes; Weak-acid salts; Transport; Hydrolysis; Modelling

1. Introduction

The understanding of electrodialysis (ED) of solutions containing weak electrolytes presents certain problems because of the hydrolysis reactions coupled with the transport. However, there are many examples where the knowledge of this process is important. The removal of weak electrolytes from natural waters during the production of drinking and especially deionised water (electrodeionisation) is difficult due to their small degree of dissociation and the competition with strong-electrolyte ions. When treating solutions containing amino acids, sometimes the aim is to remove the mineral salts and to prevent the amino acid leakage through the membranes. In facilitated transport, chemical reactions between the moving species largely determine the course of the process.

From a sufficiently general point of view, the above-mentioned problems are scientifically related to a branch of kinetics which is the ion transport coupled with homogeneous chemical reactions. The classical electrochemical approach [1] to the problem was developed later for membrane systems in the case of passive [2] or facilitated diffusion [3–6] and electromigration [7,8] of weak-electrolyte species. The role of electric field and mechanism of catalysis of the "water splitting" reaction at membrane | solution interface have been investigated experimentally and theoretically [9–13]. However, the coupling between the electrodiffusion of weak-acid ions and their hydrolysis reactions is not studied sufficiently.

The case of (bi)carbonate ion transport is chosen for the present theoretical analysis because of its relative simplicity and practical interest (ED of natural waters). Several known experimental facts [14–17] need a more comprehensive explanation than that one can find in the literature. It is known that during the ED of carbonate

* Corresponding author. Tel.: +33-46-714-9110; fax: +33-46-714-9119.
E-mail addresses: v_nikonenko@hotmail.com (V. Nikonenko), v_nikonenko@hotmail.com (K. Lebedev), jose.a.manzanares@uv.es (J.A. Manzanares), gerald.pourcelly@iemm.univ-montp2.fr (G. Pourcelly).
[1] Tel.: +7-8612-69-9573; fax: +7-8612-69-9517.
[2] Tel.: +34-96-354-3119; fax: +34-96-354-3385.

0013-4686/03/$ - see front matter © 2003 Elsevier Ltd. All rights reserved.
doi:10.1016/S0013-4686(03)00485-7

and bicarbonate containing solutions, the pH of the depleted solution decreases and that of the concentrated one increases, even when the current density is lower than the limiting one. Another interesting phenomenon is the growth of the water dissociation rate at an anion-exchange membrane (AEM) interface, at overlimiting currents, when adding carbonates (or bicarbonates) into the NaCl solution adjoining the membrane.

The formulation of the problem considered in this paper is based on the solution of the Nernst–Planck equations in a membrane system composed of three layers, namely, the membrane and the two diffusion boundary layers (DBL) [18–20]. The assumptions of local chemical and thermodynamic equilibrium, as well as local electroneutrality are accepted, as it is often done in the theoretical description of similar phenomena [2,4,5,19,20]. However, the eventual deviations from local electroneutrality and chemical equilibrium are also discussed in the present study.

2. Theory

2.1. System description

Two identical solutions of $NaHCO_3$ and H_2CO_3 are separated by an AEM. Their pH is considered to be neutral or acidic (pH < 8), so that the concentration of CO_3^{2-} ions is negligible in the bulk solutions. The composition of these solutions is specified by the pH and the Na^+ ion concentration, pH^b and c^b_{Na}.

The AEM is modelled as a homogeneous phase with a molar concentration c_m of univalent fixed charge groups. This concentration is considered to be large compared with the ionic strength of the external solutions, so that the membrane is strongly charged and the Na^+ ions are considered to be completely excluded from the membrane phase. Due to this Donnan coion exclusion [21], the concentration of H^+ ions in the membrane is lower than in the external solution, hence the membrane phase becomes more basic than the external solutions and the dissociation equilibria:

$$H_2CO_3 \Leftrightarrow HCO_3^- + H^+ \quad (1)$$

$$HCO_3^- \Leftrightarrow CO_3^{2-} + H^+ \quad (2)$$

get displaced towards the formation of CO_3^{2-} ions inside the membrane. Also, the water dissociation equilibrium:

$$H_2O \Leftrightarrow OH^- + H^+ \quad (3)$$

has to be taken into account because the concentration of OH^- ions in the membrane phase might become significant. It is then concluded that this transport problem involves six different species, H_2CO_3, HCO_3^-, CO_3^{2-}, OH^-, H^+ and Na^+, which will be referred to by subscripts 0–5, respectively. For sufficiently diluted solutions, such as natural waters, the activity coefficients are approximately equal to one, and the thermodynamic constants (at 25 °C) of the above equilibria can be written as:

$$K_1 = c_1 c_4 / c_0 = 4.5 \times 10^{-7} \text{ M} \quad (4)$$

$$K_2 = c_2 c_4 / c_1 = 4.8 \times 10^{-11} \text{ M} \quad (5)$$

$$K_w = c_3 c_4 = 1.0 \times 10^{-14} \text{ M}^2 \quad (6)$$

where c_i is the molar concentration of species i. Equations (4)–(6) are considered to be valid throughout the whole membrane system, which requires these reactions to be much faster than the transport processes (see Appendix A).

When an electric current density i is driven through the AEM, concentration polarisation develops. It is considered that HCO_3^- ions flow in the positive direction of the coordinate axis x, and hence i is negative. The concentration changes are assumed to take place inside two DBL of thickness δ flanking the membrane. The layer on the positive side of the AEM (in relation to the x axis) becomes concentrated in HCO_3^- and other ions and the pH increases there. The layer on the negative side of the AEM becomes depleted in HCO_3^- and other ions, and the pH decreases there. These layers are denoted hereafter, as the depleted and concentrated DBLs. Obviously, the extent of the pH changes, and hence the displacement of the dissociation equilibria (1)–(3) depends on the electric current density.

2.2. Transport in the membrane phase

The steady-state problem under consideration is quite complicated because it involves six different species, which are transported by diffusion and migration across a three-layer membrane system and participate in the homogeneous chemical reactions described by Eqs. (1)–(3). Several simplifying assumptions are, therefore, introduced to make the problem more tractable.

Since Na^+ ions are not involved in any reaction, their flux density is constant throughout the system. Moreover, given that the AEM is strongly charged, it can be assumed that it shows ideal permselectivity and, therefore, that the flux density of Na^+ ions vanishes everywhere.

It is generally accepted that the transport of counter-ions inside charged membranes takes place mostly by migration, and therefore, concentration gradients can be often neglected inside the membrane phase. The flux density $\bar{j}_i$ of species i inside the membrane can then be approximated by:

$$\bar{j}_i = \frac{\bar{t}_i i}{z_i F} \quad (7)$$

where $\bar{t}_i = z_i^2 \bar{D}_i \bar{c}_i / \Sigma_j z_j^2 \bar{D}_j \bar{c}_j$, $\bar{D}_i$, and z_i are the transport

number, the diffusion coefficient and the charge number of species i, respectively, F is the Faraday constant, and overbars denote membrane phase. There is no hydrostatic or osmotic pressure gradient in the membrane; hence the volume flow is not considered.

In the case of two competitive counterions, Eq. (7) is justified by three-layer models [18–20] treating the transport with the Nernst–Planck equations in the membrane and two adjoining DBLs. When the electrodiffusion resistance of the membrane is relatively high (i.e. the parameter $r=(D_i c_i d)/(\bar{D}_i \bar{c}_i \delta)$ is higher than 2), the counter-ion concentration profiles have a Γ-shaped form [19,20]. In most of the membrane volume, the internal concentrations of the counter-ions are constant and determined by the depleted surface solution (from which they enter the membrane); only a thin membrane layer adjacent to the concentrated surface solution feels the influence of this solution.

As already mentioned, the positively charged groups fixed to the membrane exclude the H^+ ions and displace the equilibrium shown in Eq. (2) towards the formation of CO_3^{2-} ions. It thus turns out to be that not only H^+ and Na^+ ions, but also H_2CO_3 molecules are absent inside the membrane. The internal concentrations of the counter-ions HCO_3^-, CO_3^{2-}, and OH^- must satisfy the local electroneutrality assumption:

$$\sum_i z_i \bar{c}_i + c_m = 0 \tag{8}$$

and it is assumed that they can be determined from the condition of thermodynamic equilibrium with the depleted surface solution.

The position of the membrane | depleted solution interface is denoted as $x=0$. The concentrations of HCO_3^- and CO_3^{2-} ions at both sides of the interface can be related by the condition of continuity of their electrochemical potentials:

$$\bar{c}_i = k_i c_i(0) \mathrm{e}^{-z_i F \Delta\phi_D(0)/RT} \tag{9}$$

where $\Delta\phi_D(0)=\bar{\phi}(0)-\phi(0)$ is the Donnan potential at this interface, k_i is the partition coefficient of species i, R is the gas constant, and T is the absolute temperature. Eliminating $\Delta\phi_D(0)$ from Eq. (9) for HCO_3^- and CO_3^{2-} ions, it is obtained that:

$$\frac{\bar{c}_2}{(\bar{c}_1)^2} = \frac{k_2 c_2(0)}{[k_1 c_1(0)]^2} = K_{21} \frac{c_2(0)}{[c_1(0)]^2}. \tag{10}$$

The ratio $K_{21}=k_2/k_1^2$ needs then to be known for the determination of $\bar{c}_1$ and $\bar{c}_2$ from Eqs. (8) and (10). Since $\bar{c}_3 \ll c_m$, the concentration of the OH^- ions inside the membrane can be calculated from Eqs. (5) and (6) as $\bar{c}_3 = \bar{c}_2 \bar{K}_w / \bar{c}_1 \bar{K}_2$. Note that when partition coefficients k_i are introduced, the equilibrium constants of the chemical equilibria (1)–(3) take the values $\overline{K} = K \prod_i k_i^{\nu_i}$ in the membrane phase, where ν_i is the stoichiometric coefficient of species i.

The electrochemical equilibrium established at the membrane | concentrated solution interface, which is denoted as $x=d$, is only relevant to the proposed simplified approach in relation to its contribution to the electric potential drop across the system. The Donnan potential at this interface, $\Delta\phi_D(d)=\bar{\phi}(d)-\phi(d)$, can be obtained from an equation similar to Eq. (9), and the sum of the interfacial potential drops can be calculated as:

$$\Delta\phi_D(0) + \Delta\phi_D(d) \approx \frac{RT}{F} \ln \frac{c_1(d)}{c_1(0)}. \tag{11a}$$

The potential drop inside the membrane is rather small and approximately ohmic. Thus, under the assumption of zero concentration gradients, it can be estimated as:

$$\Delta\bar{\phi} = \bar{\phi}(d) - \bar{\phi}(0) \approx -\frac{RT}{F^2} \frac{id}{\sum_j z_j^2 \bar{D}_j \bar{c}_j} \tag{11b}$$

where d is the membrane thickness.

2.3. Transport in the concentrated DBL

The concentrated DBL extends from $x=d$ to $d+\delta$. Even though the increase in concentration of HCO_3^- ions raises the pH in this layer, it can still be assumed that the concentration of CO_3^{2-} ions is negligible when the bulk solution has neutral or moderately acidic pH. In this case, the local electroneutrality condition can be approximated by:

$$c_1 \approx c_5 \tag{12}$$

and, since $j_5 \approx 0$, this implies that:

$$\frac{F}{RT}\frac{d\phi}{dx} \approx -\frac{d \ln c_5}{dx} \approx -\frac{d \ln c_1}{dx}. \tag{13}$$

The flux density of HCO_3^- ions is then given by;

$$j_1 = -2D_1 \frac{dc_1}{dx} \approx -\frac{i}{F} \tag{14}$$

The HCO_3^- ion concentration profile in the concentrated DBL is linear and the interfacial concentration $c_1(d)$ is determined by:

$$c_1(d) = c_1^b (1 + i/i_L) \tag{15}$$

where $i_L = -2FD_1 c_1^b/\delta < 0$ would be the electrodiffusion limiting current density in the case of a non-reactive 1:1 binary electrolyte solution; note that in the present reactive system $c_1(0)$ is different from zero when $i=i_L$.

The potential drop in this layer can be obtained from Eq. (13) as:

$$\Delta\phi_c = \phi(d+\delta) - \phi(d) = \frac{RT}{F}\ln\frac{c_1(d)}{c_1^b}. \quad (16)$$

2.4. Transport in the depleted DBL

The depleted DBL extends from $x = -\delta$ to 0, and the solution of the transport equations needs to be accurate in this layer because the homogeneous reactions (1)–(3) are expected to proceed at a significant rate in this layer. The flux density of species i is given by the Nernst–Planck equation:

$$j_i = -D_i\left(\frac{dc_i}{dx} + z_i c_i \frac{F}{RT}\frac{d\phi}{dx}\right) \quad (17)$$

where the electric potential gradient $d\phi/dx$ can be determined from the local electroneutrality assumption:

$$\sum_i z_i c_i = 0 \quad (18)$$

as:

$$\frac{F}{RT}\frac{d\phi}{dx} = -\frac{\sum_i z_i j_i/D_i}{\sum_j z_j^2 c_j}. \quad (19)$$

Since the transported species participate in chemical reactions, their steady-state flux densities are position dependent. It is possible, however, to calculate them from the following five equations; remember that $j_5 \approx 0$. The fast chemical reaction assumption (see Appendix A) allows the following relations to be derived from Eqs. (4)–(6) and (17)

$$\frac{j_1}{D_1 c_1} + \frac{j_4}{D_4 c_4} = \frac{j_0}{D_0 c_0} \quad (20)$$

$$\frac{j_2}{D_2 c_2} + \frac{j_4}{D_4 c_4} = \frac{j_1}{D_1 c_1} \quad (21)$$

$$\frac{j_3}{D_3 c_3} + \frac{j_4}{D_4 c_4} = 0. \quad (22)$$

The electric current density:

$$i = F\sum_i z_i j_i = F\sum_i z_i \bar{j}_i \quad (23)$$

and the total carbon flux density;

$$j_T = j_0 + j_1 + j_2 = \bar{j}_0 + \bar{j}_1 + \bar{j}_2 \quad (24)$$

are both independent of position x because chemical reactions conserve electric charge and the total carbon amount. From Eq. (7), and neglecting $\bar{j}_0$ because the H_2CO_3 concentration is negligible in the membrane, the total carbon flux density can be written as:

$$j_T = -\left(\bar{t}_1 + \frac{\bar{t}_2}{2}\right)\frac{i}{F}. \quad (25)$$

Finally, the potential drop $\Delta\phi_d$ across the depleted DBL can be obtained from the Nernst–Planck equation and the fact that $j_5 \approx 0$ as:

$$\Delta\phi_d = \phi(0) - \phi(-\delta) = \frac{RT}{F}\ln\frac{c_5^b}{c_5(0)} \quad (26)$$

where the condition $c_5(-\delta) = c_5^b$ has been used.

2.5. Solution procedure

For every value of the electric current density i, and starting from $x = -\delta$, the transport equations are integrated numerically by using a second-order Euler finite-difference formula. A shooting procedure is used to determine j_T. Starting with a guess value of j_T, the integration is performed up to the membrane | solution interface at $x = 0$. Then, the molar concentrations in the membrane phase are obtained from Eqs. (8) and (10). The transport numbers $\bar{t}_1$ and $\bar{t}_2$ are calculated, and Eq. (25) is used to estimate a new value of j_T. The procedure is repeated until Eq. (25) is satisfied to the accuracy required. Then the potential drops are calculated from Eqs. (11a), (11b), (16) and (26) and the total potential drop U across the membrane system is evaluated as their sum:

$$U = \Delta\phi_d + \Delta\phi_D(0) + \Delta\bar{\phi} + \Delta\phi_D(d) + \Delta\phi_c. \quad (27)$$

Thus, the transport numbers in the membrane, the total potential drop and the distribution of concentrations, flux densities and electric potential are calculated as functions of the current density. The diffusion coefficients D_i and $\bar{D}_i$, the ratio of partition coefficients K_{21}, the fixed charge concentration c_m, the bulk solution concentrations c_i^b, and the thickness δ of the DBLs and d of the membrane are considered as fixed parameters. Most of the results presented below have been obtained with the following parameter values, which are typical for an AEM in contact with drinking water: $2D_0 = D_1 = D_2 = D_3/5 = D_4/10 = D_5 = 10^{-5}$ cm^2 s^{-1}; $c_1^b \approx c_5^b = 10$ mM; $pH^b = 7$, $\bar{D}_i = 10^{-6}$ cm^2 s^{-1}, $K_{21} = 1$; $k_i = 1$; $c_m = 1$ M, $d = 0.05$ cm, and $\delta = 0.01$ cm. The bulk concentrations of H_2CO_3 and CO_3^{2-} under these conditions are $c_0^b = 2.22$ mM and $c_2^b = 0.87$ μM.

3. Results and discussion

One interesting result, which is common to both underlimiting and overlimiting current regimes, is that, under the conditions considered in the present calculations, the contribution of OH^- ions to the electrical current transport inside the membrane is negligible. Therefore, it can be considered that there are only two charge carriers, HCO_3^- and CO_3^{2-}, in the membrane phase and their transport numbers satisfy the relation

$\bar{t}_1 + \bar{t}_2 \approx 1$. Then, according to Eq. (25), the total carbon flux density is $j_T = -i/\tau_1 F$ where $\tau_1 = 2/(1+\bar{t}_1) > 1$. The variable τ_1 is defined as the ratio between the HCO_3^- ion flux density in the DBL and the total carbon flux density, $\tau_1 \equiv j_1/j_T$. Table 1 shows the relations between flux densities of the different species in the DBL and in the membrane phase, the total carbon flux j_T and the electric current density i for the cases $i/i_L < 1$ and $i/i_L > 1$.

3.1. Transport mechanism in the underlimiting current regime

The transport mechanism taking place in the underlimiting current regime, $i/i_L < 1$, is schematically shown in Fig. 1 and has been denoted as mechanism A. The description of transport in the depleted DBL closely resembles that presented in Section 2.3 for the concentrated DBL. The majority ions are HCO_3^- and Na^+ and the local electroneutrality condition can be approximated by $c_1 \approx c_5$. Their flux densities are $j_5 \approx 0$ and $j_1 \approx -i/F$, the concentration profiles are linear, the interfacial concentrations are $c_5(0) \approx c_1(0) = c_1^b(1-i/i_L)$, and the potential drop is $\Delta\phi_d \approx -(RT/F)\ln(1-i/i_L)$.

In addition to the transport of HCO_3^- and Na^+ ions, there is also a transport of H_2CO_3 molecules in the DBL. Since $j_T \approx j_0 + j_1 = -i/\tau_1 F < -i/F = j_1$ the flux density of H_2CO_3 molecules must take place in opposite direction to the HCO_3^- ions flux density. Indeed, it can be easily shown that $j_0 = j_T - j_1 = -(\tau_1 - 1)j_T < 0$, that is, the H_2CO_3 molecules move from the membrane towards the depleted DBL. It should be observed, however, that the flux density of H_2CO_3 molecules in the membrane phase is negligible.

In the membrane phase there are two charge carriers, HCO_3^- and CO_3^{2-}, moving from the surface facing the depleted DBL to that facing the concentrated DBL. It should be observed that the flux density of CO_3^{2-} ions in the depleted DBL is practically zero, and that the flux density of HCO_3^- anions in the membrane phase is lower than in the depleted DBL (that is, $\bar{j}_1 \approx \bar{t}_1 j_1 < j_1$). This means that only a fraction $\bar{t}_1 < 1$ of the HCO_3^- anions that reach the depleted interface of the membrane cross it, and the rest of the anions must undergo a chemical transformation into CO_3^{2-} and H_2CO_3.

Referring the flux densities to j_T, the flux density of HCO_3^- anions in the membrane phase is $\bar{j}_1 \approx (2-\tau_1)j_T$ and the fraction of anions that undergo a chemical transformation is $j_1 - \bar{j}_1 = 2(\tau_1 - 1)j_T$. Half of them, that is, a flux density $(\tau_1 - 1)j_T$ crosses the membrane as CO_3^{2-} ions, while an equal amount goes back into the depleted DBL as H_2CO_3 molecules. These important changes in the flux densities of these three species take place in a very narrow interfacial reaction zone (i.e. a region of thickness much smaller than δ, and hence taken to be zero). In the membrane side of this reaction zone, the concentration of CO_3^{2-} and OH^- ions is relatively high, and so is the pH. Contrarily, in the DBL side of this reaction zone, the concentration of H_2CO_3 and H^+ is high, and the pH is low. The high interfacial concentration of H^+ ions and H_2CO_3 molecules explains the direction of the flux density of H_2CO_3 molecules in the depleted DBL.

3.2. Transport mechanism in the overlimiting current regime

The present model allows the current density to be higher than its limiting value, where the concentration of Na^+ ions becomes negligible in a depleted solution region close to the interface. Hence, other positive ions (H^+ ions) should compensate the charge of anions in this region, and an additional transport mechanism must occur. This mechanism has been denoted as mechanism B in Fig. 1.

When $i/i_L > 1$, the depleted DBL can be divided in two regions, in addition to the above-mentioned interfacial reaction zone, the thickness of which is supposed zero in this model. The properties of the outer region, $-\delta < x < -\delta^r$, are similar to those of the whole DBL, $-\delta < x < 0$, in the underlimiting current regime, $i/i_L < 1$. In this outer DBL region, the reaction rates are

Table 1
Flux densities of carbonic acid, carbonic anions and hydrogen ions in the different regions of the membrane system in the underlimiting and overlimiting current regimes

Regime	Species	DBL (outer region)	DBL (reaction zone)	Membrane
$i/i_L < 1$	H_2CO_3	$j_0 \approx -(\tau_1 - 1)j_T$		$\bar{j}_0 \approx 0$
	HCO_3^-	$j_1 \approx -i/F = \tau_1 j_T$		$\bar{j}_1 \approx -\bar{t}_1 i/F = (2-\tau_1)j_T$
	CO_3^{2-}	$j_2 \approx 0$		$\bar{j}_2 \approx -(\bar{t}_2/2)i/F = (\tau_1 - 1)j_T$
$i/i_L > 1$	H_2CO_3	$j_0 \approx -(\tau_1 - 1)j_T$	$j_0^r \approx (1 - \tau_1 t_1^r)j_T$	$\bar{j}_0 \approx 0$
	HCO_3^-	$j_1 \approx -i/F = \tau_1 j_T$	$j_1^r \approx -t_1^r i/F = \tau_1 t_1^r j_T$	$\bar{j}_1 \approx -\bar{t}_1 i/F = (2-\tau_1)j_T$
	CO_3^{2-}	$j_2 \approx 0$	$j_2^r \approx 0$	$\bar{j}_2 \approx -(\bar{t}_2/2)i/F = (\tau_1 - 1)j_T$
	H^+	$j_4 \approx 0$	$j_4^r \approx t_4^r i/F$	$\bar{j}_4 \approx 0$

The conditions $j_T = j_0 + j_1 + j_2$ and $-i/F \approx j_1 + 2j_2 - j_4$ are satisfied in every region. Variables τ_1, t_1^r and t_4^r are defined as follows: $\tau_1 \equiv j_1/j_T$, $t_1^r \equiv -Fj_1^r/i$, and $t_4^r \equiv -Fj_4^r/i$.

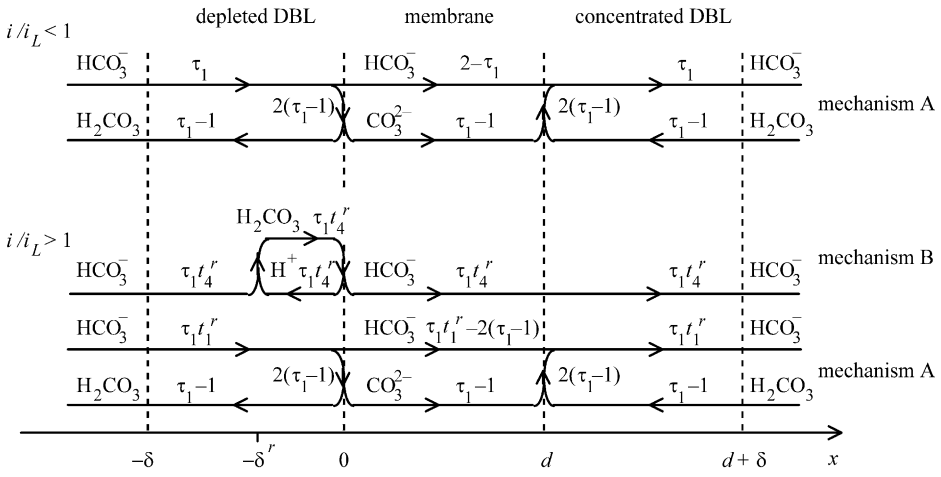

Fig. 1. Schematic representation of the electrodiffusion-reaction mechanisms that operate in the underlimiting and overlimiting current regimes. The contributions of these mechanisms to the flux densities of the species involved as shown in j_T units. For instance, the value τ_1-1 corresponding to the CO_3^{2-} ions in the membrane phase means that $\bar{j}_2/j_T=\tau_1-1$.

negligible, HCO_3^- and Na^+ are the majority ions and the local electroneutrality condition can be approximated by $c_1\approx c_5$. Their flux densities are $j_5\approx 0$ and $j_1\approx -i/F$, and their linear concentration profiles are given by $c_5(x)\approx c_1(x)=c_1^b[1-(i/i_L)(1+x/\delta)]$. In this region the H_2CO_3 flux density is directed towards the outer limit of the depleted DBL because $j_0\approx j_T-j_1=-(\tau_1-1)j_T<0$.

In the inner region, $-\delta^r<x<0$, the concentration of Na^+ ions is negligible, the majority ions are HCO_3^- and H^+, and the local electroneutrality condition can be approximated by $c_1\approx c_4$. The reason why the concentration of HCO_3^- ions does not vanish in this region is because reaction (1) proceeds at a significant rate r_1. Hence, this region is denoted as the DBL reaction zone. From the condition $c_5(-\delta^r)\approx 0$ and the above linear concentration profile, the thickness of the reaction zone can be estimated as $\delta^r\approx\delta(1-i_L/i)$, which increases with the current density $|i|$.

In the reaction zone, the HCO_3^- and H^+ ions move in opposite directions to carry the electric current density and their flux densities satisfy the equation $j_4^r-j_1^r\approx i/F$. These flux densities can be conveniently expressed as $j_1^r=-t_1^r i/F$ and $j_4^r=-t_4^r i/F$, where the local effective transport numbers in the reaction zone satisfy the relation $t_1^r+t_4^r=1$. Since the flux density of HCO_3^- ions is $j_1=\tau_1 j_T$ in the outer region of the DBL and $j_1^r=\tau_1 t_1^r j_T=\tau_1 j_T-\tau_1 t_4^r j_T$ in the inner region (transport mechanism A), it must be concluded that a flux density $\tau_1 t_4^r j_T$ of HCO_3^- ions must recombine with H^+ ions moving in the opposite direction to form H_2CO_3 molecules (transport mechanism B). Then, in the vicinity of the zone boundary, $x\approx-\delta^r$, the rate of reaction (1) is $r_1=-dj_0/dx\approx dj_1/dx\approx dj_4/dx<0$ and the concentration of H_2CO_3 molecules must show a maximum.

Interestingly, as the membrane | solution interface located at $x=0$ is approached, the rate r_1 of reaction (1) changes from negative to positive values. In this region, the electric field is very large, the electric current is mostly driven by H^+ ions (note that $D_4\approx 10D_1$), and there is a large flux of H_2CO_3 molecules towards the membrane. However, since these molecules cannot cross the interface, there must be a net dissociation of H_2CO_3 molecules into HCO_3^- and H^+ ions and, therefore, $r_1-dj_0/dx\approx dj_1/dx\approx dj_4/dx>0$. The HCO_3^- ions cross the membrane and contribute a fraction $\tau_1 t_4^r j_T$ to $\bar{j}_1\approx(2-\tau_1)j_T$. The H^+ ions are transported towards the depleted DBL and their flux density is $j_4^r=t_4^r i/F=-\tau_1 t_4^r j_T$ (note that the transport numbers t_1^r and t_4^r are position dependent).

The difference between $\bar{j}_1\approx(2-\tau_1)j_T$ and the contribution $\tau_1 t_4^r j_T$ mentioned above is associated to the transport mechanism A and the flux density $j_1^r=\tau_1 t_1^r j_T$ in the inner region of the DBL. When the HCO_3^- anions reach the interface from the depleted DBL, a fraction of them must undergo a chemical transformation through reaction (2) into CO_3^{2-} ions, which cross the membrane, and H_2CO_3 molecules, which go back into the depleted DBL. Since $\bar{j}_2\approx(\tau_1-1)j_T$, and given the reaction stochiometry, the fraction of j_1^r that undergo the chemical transformation is $2(\tau_1-1)j_T$, and the rest of the HCO_3^- anions cross the interface and add to the $\tau_1 t_4^r j_T$ coming from mechanism B to make the total $\bar{j}_1\approx(2-\tau_1)j_T$. Table 1 shows the total flux densities as the sum of transport mechanisms A and B (compare Table 1 and Fig. 1).

Note, finally that the rates of reactions (1) and (2) are very large in the interfacial reaction zone of negligible thickness, and they both contribute to make maximum the concentration of H^+ ions in the DBL region close to the interface $x=0$. These ions move towards the depleted solution, thus decreasing the pH of this solution.

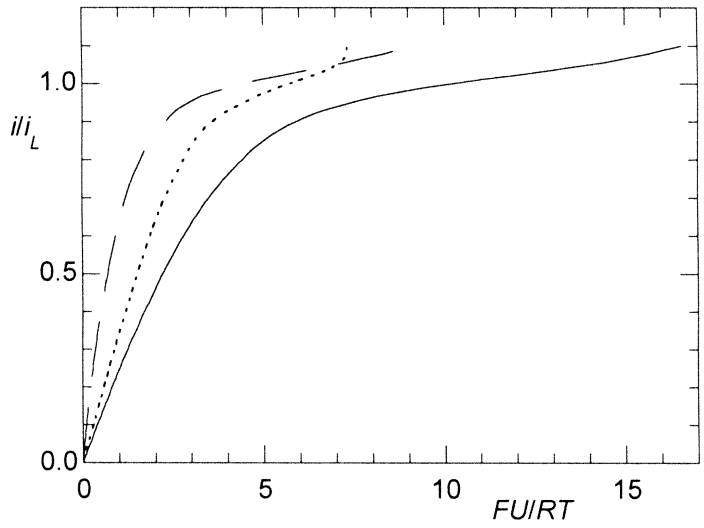

Fig. 2. Current–voltage curves showing the contributions $\Delta\phi_d$ (— — —, Eq. 26) and $U-\Delta\phi_d=\Delta\phi_D(0)+\Delta\bar{\phi}+\Delta\phi_D(d)+\Delta\phi_c$ (- - - -, Eqs. 11a, 11b, and 16) to the total potential drop U (—, Eq. 27). The parameters values used in the calculations are; $2D_0=D_1=D_2=D_3/5=D_4/10=D_5=10^{-5}$ cm^2 s^{-1}; $c_1^b\approx c_5^b=10$ mM; pH$^b=7$, $\bar{D}_i=10^{-6}$ cm^2 s^{-1}, $k_i=1$; $c_m=1$ M, $d=0.05$ cm, and $\delta=0.01$ cm.

3.3. Current–voltage curve

Fig. 2 shows the current–voltage curves of the system. Most of the potential drop across the membrane system is expected to occur in the depleted DBL under overlimiting current conditions because, according to Eq. (26), $c_5(0)$ becomes negligible then. Thus, the total potential drop U has been decomposed in two contributions, namely, the potential drop $\Delta\phi_d$ in the depleted DBL given by Eq. (26), and the other four contributions $\Delta\phi_D(0)+\Delta\bar{\phi}+\Delta\phi_D(d)+\Delta\phi_c$ shown in Eq. (27).

In a non-reactive 1:1 binary electrolyte solution, the potential drops across the whole membrane system and in the depleted DBL are given by $U^{\text{bin}}=(RT/F)\,\text{arctanh}(i/i_L)$ and $\Delta\phi_d^{\text{bin}}=-(RT/F)\ln(1-i/i_L)$, respectively, and both diverge when $i\to i_L$. In the present system, however, since the electric current can also be transported by H^+ ions in the depleted DBL when $i/i_L>1$, the potential drops U and $\Delta\phi_d$ are smaller U^{bin} and $\Delta\phi_d^{\text{bin}}$, respectively, and do not diverge.

3.4. Transport numbers

Fig. 3 shows the transport number of HCO_3^- ion in the membrane phase and evidences the different transport mechanisms discussed in Sections 3.1 and 3.2. The transport number $\bar{t}_1$ increases with increasing $|i|$ when $i/i_L<1$, while it decreases with increasing $|i|$ when $i/i_L>1$. By writing Eq. (10) in the form $\bar{c}_2/(\bar{c}_1)^2=K_{21}K_2/K_1c_0(0)$ and differentiating this and Eq. (8), it is easy to show that $d\bar{c}_2/dc_0(0)<0$ which means that $\bar{t}_1$ increases with increasing $c_0(0)$. In the underlimiting current regime, the H_2CO_3 molecules are produced at the depleted interface, the local pH (at the DBL side of the interface) is low. The flux density of H_2CO_3 molecules towards the bulk solution is $j_0\approx(1-\bar{t}_1)i/2F=-D_0[c_0(0)-c_0^b]/\delta$ and, therefore, $c_0(0)$ increases with increasing $|i|$, thus explaining the observed trend for $\bar{t}_1$. The concentration of CO_3^{2-} ions in the membrane is small and decreases with increasing current density $|i|$, and so does $\bar{t}_2$.

The above arguments also imply that the observed decrease in $\bar{t}_1$ with increasing $|i|$ when $i/i_L>1$ must correspond to a decrease in $c_0(0)$. In this regime, mechanism B becomes operative and consumes H_2CO_3 molecules at the depleted interface, thus decreasing their concentration there. This mechanism increases the local pH (at both sides of the interface) and hence the concentration of CO_3^{2-} ions inside the membrane. As a result, $\bar{t}_1$ decreases with increasing $|i|$ (Fig. 3).

Note also that the Donnan potential drop at the membrane | depleted solution interface $\Delta\phi_D(0)=\bar{\phi}(0)-\phi(0)$ becomes large (and positive) when $i/i_L>1$. Thus, the concentration of the double charged CO_3^{2-} ions becomes large inside the membrane even though their

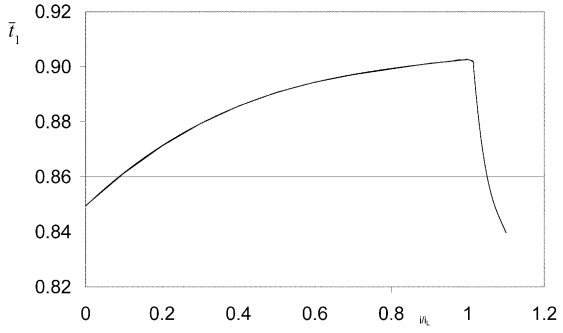

Fig. 3. Transport number $\bar{t}_1$ of HCO_3^- ions in the membrane as a function of i/i_L. The transport numbers of Na^+, H^+, and OH^- ions in this phase are negligible, while that of CO_3^{2-} ions is approximately equal to $1-\bar{t}_1$. Parameter values are the same as in Fig. 2.

external concentration is very small. For instance, when $i/i_L = 1.1$, for a membrane system characterised by the parameters specified in Section 2.5, $\Delta\phi_D(0) = 270$ mV, the transport number of CO_3^{2-} ions in the membrane phase is $\bar{t}_2 \approx 0.234$, the internal concentration is $\bar{c}_2 = 66.08$ mM and the external concentration (close to the interface) is only $c_2(0) = 48.62 \times 10^{-12}$ M, to be compared with the concentrations of HCO_3^- and H^+ ions at this same location which are $c_1(0) = 23.54$ μM and $c_4(0) = 23.13$ μM, respectively.

3.5. Concentration profiles and flux densities in the depleted DBL

Fig. 4a shows the calculated concentration profiles corresponding to $i/i_L = 0.2$. As described in Section 3.1, the concentration profiles of the majority ions are linear and their interfacial concentration is determined by $c_5(0) \approx c_1(0) = c_1^b(1 - i/i_L)$. At this current density $i/i_L = 0.2$, the transport number of the HCO_3^- anions in the membrane is $\bar{t}_1 = 0.872$ and, therefore, the flux density of H_2CO_3 molecules towards the bulk solution is $j_0 \approx (1 - \bar{t}_1)i/2F = 0.0128 i_L/F < 0$ Since this flux is only driven by diffusion, the concentration of H_2CO_3 molecules, and hence that of H^+ ions, must be maximum at $x = 0$. It is observed that the concentration profile of H_2CO_3 in the depleted DBL is approximately linear and its flux density is constant throughout the DBL (Fig. 5a), it can be concluded that the rate of reaction (1) is negligible in the depleted DBL (outside the interfacial reaction zone).

Fig. 4b and Fig. 5b show the concentration profiles and flux densities for the case $i/i_L = 1.05$. The transport number of the HCO_3^- anions in the membrane is $\bar{t}_1 = 0.859$, as shown in Fig. 3. The thickness of the DBL reaction zone (i.e. the region where the concentration profiles are non-linear and the flux densities vary with position) is of the order of δ/10; in rough agreement with the estimation $\delta^r \approx \delta(1 - i_L/i) \approx \delta/20$.

It is important to remember that the present study makes use of the local electroneutrality assumption. Even though the ionic concentrations close to the membrane | depleted DBL interface are still of the order of tens or hundreds of μM when $1 < i/i_L < 1.1$, the presence of a large electric field in this region might indicate that this assumption is no longer valid and the Poisson equation should be used instead. Therefore, the standard test of local electroneutrality assumption has been carried out. This test requires evaluating the

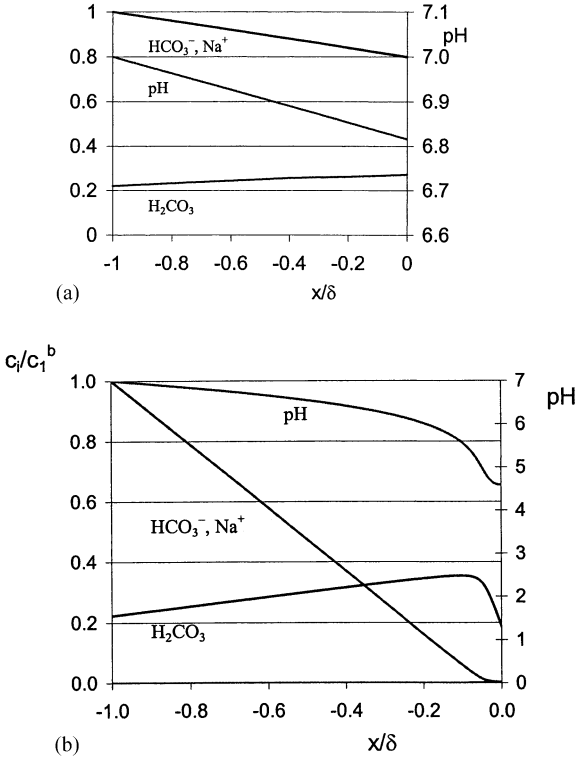

Fig. 4. Concentration profiles of the majority species (H_2CO_3, HCO_3^-, and Na^+) and pH variation with x in the depleted DBL; (a) in the underlimiting ($i/i_L = 0.2$) and (b) overlimiting ($i/i_L = 1.05$) current regimes. Parameter values are the same as in Fig. 2.

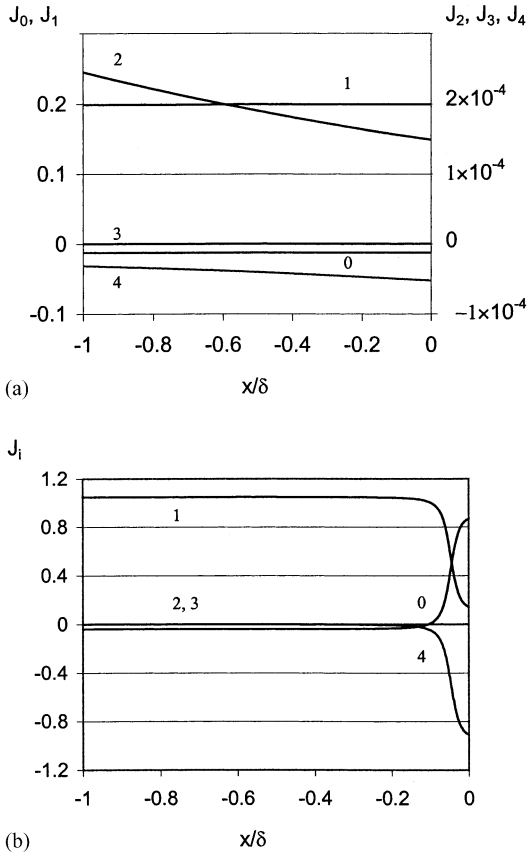

Fig. 5. Position dependence of the dimensionless flux of H_2CO_3 molecules, $J_0 = Fj_0/i_L$, and HCO_3^- (1), CO_3^{2-} (2), OH^- (3), and H^+ (4) ions, $J_i = z_i F j_i / i_L$, in the depleted DBL; (a) in the underlimiting ($i/i_L = 0.2$) and (b) overlimiting ($i/i_L = 1.05$) current regimes. Note the two ordinate scales used in figure (a). Parameter values are the same as in Fig. 2.

residual space charge density associated to the electric potential profile, which is obtained as:

$$\rho = \varepsilon \frac{d^2\phi}{dx^2} = 2Fc_1^b \kappa_D^{-2} \frac{F}{RT} \frac{d^2\phi}{dx^2} \quad (28)$$

where ϕ is the electric potential calculated from the local electroneutrality assumption, $\kappa_D = (2F^2 c_1^b/\varepsilon RT)^{1/2}$ is the reciprocal Debye length, and ε is the dielectric permittivity of the solution. The validity of the local electroneutrality assumption requires that this residual space charge density must be smaller than $F\,\Sigma_j z_j^2 c_j$ throughout the system. It is observed that when $i/i_L \approx 1.1$ this is no longer true in the region close to the interface where $r_1 > 0$. For higher currents, the use of the Poisson equation or the condition of quasi-uniform space charge density [22] (instead of the electroneutrality condition) would allow for a more precise calculation of the concentrations in this region [18,22,23], and this might affect the shape of the current–voltage curve in the overlimiting current regime.

Note also that the DBL thickness can change (but this change is not considered in the model) with the current due to coupled convection. The mechanism of this convection depends on the solution concentration, flow velocity and the cell geometry [20]. The gravitational convection is more probable in concentrated solutions and in cells with a great distance between the membranes [20], while the contribution of the electroconvection [24] is more important in diluted solutions and when the DBL thickness is rather small [20].

3.6. The rate of variation of the solution pH

The understanding of the mechanism of pH variation in the diluting and concentrating streams during ED of natural waters is very important because it influences the process performance. Effectively, the experimental results show that the pH of diluting stream decreases and that of the concentrating stream increases with the current [15–17]. The rate of this variation is not negligible even when the current density is significantly less than the limiting one. The decrease in the pH of the diluting stream is not favourable for the ED process because HCO_3^- ions are then transformed into non-dissociated H_2CO_3, thus becoming more difficult their removal. The increase in the pH of the concentrating stream makes more likely the precipitation of $CaCO_3$ at the membrane surface.

A simple way to analyse the pH variation in the diluting stream consists in considering this stream as a closed bulk solution of volume V and area A (parallel to the membrane) of varying composition due to the exchange of HCO_3^- and H_2CO_3 with the depleted DBL. Since Eq. (4) is valid within the bulk solution, the time variations of the concentration of the three major components of this solution satisfy:

$$\frac{d \ln c_0^b}{dt} = \frac{d \ln c_1^b}{dt} + \frac{d \ln c_4^b}{dt} \quad (29)$$

The conservation of hydrogen and carbon atoms requires that their flux across the bulk solution | depleted DBL interface equals their time variation in the bulk solution, and then:

$$(2j_0 + j_1)A = \left(2\frac{dc_0^b}{dt} + \frac{dc_1^b}{dt} + \frac{dc_4^b}{dt}\right)V \quad (30)$$

$$(j_0 + j_1)A = \left(\frac{dc_0^b}{dt} + \frac{dc_1^b}{dt}\right)V \quad (31)$$

where the flux densities j_0 and j_1 are to be evaluated at $x = -\delta$, and j_4 has been neglected because it is much smaller than j_0 and j_1. By combining Eqs. (29)–(31), and taking into account that $j_1 = -i/F$ and $c_4^b \ll c_0^b$, c_1^b, it can be shown that:

$$\frac{d \ln c_4^b}{dt} = \left(\frac{j_0}{c_0^b} - \frac{j_1}{c_1^b}\right)\frac{A}{V} = \left(\frac{J_0}{c_0^b} - \frac{i}{i_L c_1^b}\right)\frac{Ai_L}{VF} \quad (32)$$

where $J_0 \equiv j_0 F/i_L$ is the dimensionless flux of H_2CO_3 molecules across the $x = -\delta$ interface. Therefore, it is concluded that the extent of the pH variation in the diluted bulk solution depends on the current density i and the flux J_0. An analysis of the variation of J_0 with the different system parameters is presented in Fig. 6.

The flux of H_2CO_3 is due to the fact that this acid is formed inside the solution reaction zone (in the depleted DBL) and moves towards the diluting bulk solution

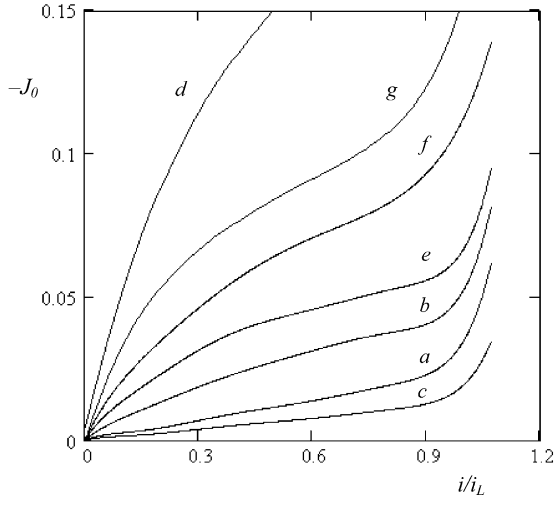

Fig. 6. Dimensionless flux of H_2CO_3 molecules, $J_0 = Fj_0/i_L$, at $x = -\delta$ as a function of i/i_L. Curve (a) has been calculated using the following parameter values $2D_0 = D_1 = D_2 = D_3/5 = D_4/10 = D_5 = 10^{-5}$ cm^2 s^{-1}; $c_1^b \approx c_5^b = 10$ mM; pH$^b = 7$; $\bar{D}_i = 10^{-6}$ cm^2 s^{-1}; $K_{21} = 1$, other $k_i = 1$; $c_m = 1$ M; $d = 0.05$ cm and $\delta = 0.01$ cm. The other curves have been calculated using the same parameter values as in the case of curve (a) except for the one specified; (b) $\bar{D}_2 = 5 \times 10^{-6}$ cm^2 s^{-1}, (c) $\bar{D}_2 = 2 \times 10^{-7}$ cm^2 s^{-1}, (d) $K_{21} = 5$, (e) pH$^b = 7.5$, (f) pH$^b = 6.5$ and (g) $c_1^b \approx c_5^b = 1$ mM.

down its concentration gradient. It should be apparent that the flux J_0 must be greater under those conditions that increase the generation rate of H_2CO_3 in the reaction zone, and hence the concentration gradient dc_0/dx. It was shown above that, when $i/i_L < 1$, the transformation of some HCO_3^- ions into H_2CO_3 and CO_3^{2-} ions in the reaction zone can be associated to the fact that CO_3^{2-} ions carry a fraction of the current density in the membrane phase. It should then be expected that an increase in $\bar{t}_2$, due to either an increase in $\bar{D}_2$ or an increase in $\bar{c}_2$, must lead to an increase in J_0. This is confirmed by the numerical results presented in Fig. 6 (compare curves a, c, e for the effect of $\bar{D}_2$, and curves c, f for the effect of K_{21}).

The generation rate of H_2CO_3 in the reaction zone can also be increased by increasing the solution pH. An increase in the external pH causes an increase in the internal pH, and hence an increase in $\bar{c}_2$. In addition, an increase in the external pH causes a decrease in the bulk H_2CO_3 concentration (at fixed c_1^b), and therefore, an increase in its concentration gradient in the depleted DBL. This is confirmed by curves b and c in Fig. 6.

The H^+ ions generation at the membrane | depleted solution interface occurs more intensively in diluted solutions. In this case the interfacial concentrations of HCO_3^- and Na^+ ions get comparable to that of H^+ ions at lower potential differences. Hence, the contribution of these ions in the charge transfer as well as the relative rate of H_2CO_3 transport into the bulk is greater. This can be illustrated by comparison of curves a and g in Fig. 6.

4. Conclusions

The model considered is based on the well known assumptions of the local electroneutrality, chemical and thermodynamic equilibrium. The account of the transport in three layers being an anion exchange membrane and two adjoining diffusion layers allowed a new insight in the understanding of the mechanism of weak-acid anions transfer through anion exchange membranes taking as example (bi)carbonate ions. The mechanism may be described as follows. Due to Donnan exclusion of H^+ ions from the membrane, the membrane interstitial solution should have a higher pH value than the external solution and be enriched with CO_3^{2-} anions. It is shown that a fraction $1-\bar{t}_1$ of the HCO_3^- anions reaching the membrane | depleted solution interface transforms to CO_3^{2-} and H_2CO_3. The former migrate across the membrane, while the latter go back into the depleted DBL towards the diluting bulk solution. Thus, during the ED of (bi)carbonate-containing solutions, the pH of the depleted solution decreases, while that of the concentrated one increases.

The theoretical analysis may help to understand which membrane parameters should be varied to change the ratio between the competitive fluxes of single charged and bi-charged anions through the membrane as well as to increase or decrease the rate of the pH variation in diluting or concentrating streams.

Acknowledgements

J.A.M. thanks the financial support from CICYT (Ministry of Science and Technology of Spain) and FEDER (Fondo Europeo de Desarrollo Regional) under project No. MAT2002-00646. K.L. thanks the University of Valencia for his visiting scientist grant. This research was also financially supported by the INTAS Aral Sea project 00-1058, by the CNRS, France, grant PICS 1811, and by the Russian Foundation of Basic Researches, grant 01-03-32171.

Appendix A

The theoretical modelling presented is based on the local chemical equilibrium assumption. The possibility of eventual deviations from this assumption is critically analysed in this appendix. These deviations may appear when the kinetic limiting current density i_k becomes comparable to the electrodiffusion limiting current density $|i_L|$. It is known [9,25] that the formation of a "normal" acid [25] (for example, the formation of H_2CO_3 as the backward recombination half-reaction (1)) is fast. This reaction takes place in the outer region of the DBL reaction zone when $i/i_L > 1$. This recombination process has a large kinetic rate constant $k_{r1} = 4.7 \times 10^{10}\ M^{-1}\ s^{-1}$ [25], and therefore, the assumption that it is not a rate-determining step is justified.

However, three rate-determining steps controlled by chemical reactions may be envisaged: the reactions of dissociation of H_2CO_3, HCO_3^- and H_2O, which occur in the very thin interfacial reaction zone.

Following Ref. [9], the kinetic limiting current density for dissociation half-reactions is evaluated as:

$$i_k = Fk_d c^* \lambda \tag{33}$$

where k_d is the dissociation rate constant, c^* is the typical concentration of the dissociation species in the interfacial reaction zone, and $\lambda \approx 2$ nm is the thickness of this zone [9]. This estimation of i_k assumes that the dissociation products are ionic and leave the reaction zone under the influence of a very strong electric field existing in this zone.

Consider first the dissociation half-reaction of Eq. (1). As shown in Fig. 1, this half-reaction takes place at $x \approx 0$ when $i/i_L > 1$. The dissociation rate constant may be calculated as [25]: $k_{d1} = K_1 k_{r1} = 2.1 \times 10^{-4}\ s^{-1}$. Using

$c_{0\ *} \approx 5$ mM, Eq. (33) yields $i_{k1} = Fk_{d1}c_{0\ *}\lambda \approx 2$ mA cm^{-2}, which is of the same order of magnitude that $|i_L|$, as estimated for $D_1 = 10^{-5}$ cm^2 s^{-1}, $c_1^b = 10$ mM, and $\delta = 10^{-2}$ cm.

The dissociation half-reaction of Eq. (2) takes place at $x \approx 0$ at all current densities. Assuming that $k_{r2} \approx k_{r1} = 4.7 \times 10^{10}$ M^{-1} s^{-1}, the dissociation rate constant can be estimated as $k_{d2} = K_2 k_{r2} \approx 2$ s^{-1}. Application of Eq. (33) with $c_{1\ *} \approx c_m = 1$ M gives $i_{k2} = Fk_{d2}c_{1\ *}\lambda \approx 0.04$ mA cm^{-2} which would lead to the conclusion that this is the rate-determining step and not the electrodiffusion through the depleted DBL. However, it is rather unlikely that the dissociation takes place as described in Eq. (2). Alternatively, the actual process occurring at $x \approx 0$ at all current densities can be described as (see Section 3.1 and Fig. 1):

$$HCO_3^- + H_2O \Leftrightarrow H_2CO_3 + OH^- \quad (34a)$$

$$HCO_3^- + OH^- \Leftrightarrow CO_3^{2-} + H_2O \quad (34b)$$

The forward rate constant of reaction (34b) (proton-transfer reaction) is known to be very large, $k_{f3b} = 6 \times 10^9$ M^{-1} s^{-1} [25], so that the formation of CO_3^{2-} ions is not rate determining provided that the forward rate step of reaction (34a) produces enough OH^- ions. This latter requirement is also satisfied because the equilibrium constant of reaction (34a) is $K_w/K_1 = 2.2 \times 10^{-8}$ M^{-1} and the backward rate constant of this reaction (being also proton-transfer one) can be approximated by $k_{b\,3a} = 6 \times 10^9$ M^{-1} s^{-1} thus yielding a large forward rate constant (of the order of 2×10^2 s^{-1}), and hence a large kinetic limiting current density (of the order of 2 mA cm^{-2}).

It should be mentioned that equilibrium between OH^- and H^+ ions and water molecules, Eq. (3), is also assumed in the model and that there is experimental evidence that the water dissociation may be slow in bulk solution and in strong acid or basic ion-exchange membranes, the rate constant being of the order of 1 s^{-1} [9–13]. However, this is not likely to introduce any kinetic limitations in the present system because of the two following facts. First, the H^+ ions that transport the electric current in the depleted DBL in the range of the currents studied, $i/i_L \leq 1.1$, do no originate from the water dissociation but from the dissociation of H_2CO_3 and HCO_3^- ions; note also that the concentration and transport number of OH^- ions in the membrane phase is always negligible. Second, it is well known that the water dissociation may be sufficiently fast in the presence of weak acidic or basic groups because it is catalysed, e.g. by weak-base amines in AEMs. The catalytic mechanism is similar to that presented in reactions (34a) and (34b) [9,11,13]. It is clear that the HCO_3^- anions present in the AEM play the same role as fixed weakly basic anions in relation to water dissociation. Reactions (34a) and (34b) explain also the experimental fact of the water "splitting" reaction acceleration by the presence of HCO_3^- anions in the depleted solution in contact with the AEM.

Finally, when evaluating reaction rates, it has to be taken into account that the electric field in the interfacial region can accelerate these reactions by at least a factor 6–50 [9–13]. This means that the kinetic limiting current densities estimated above are lower bounds, and the assumption of the local chemical equilibrium in considered cases becomes further justified.

References

[1] K.J. Vetter, Electrochemical Kinetics, Academic Press, New York, 1967.

[2] P. Ramírez, A. Alcaraz, S. Mafé, J. Pellicer, pH and supporting electrolyte concentration effects on the passive transport of cationic and anionic drugs through fixed charge membranes, J. Membr. Sci. 161 (1999) 143.

[3] A. Dindi, R.D. Noble, C.A. Koval, An analytical solution for competitive facilitated membrane transport, J. Membr. Sci. 65 (1992) 39.

[4] M. Métayer, D. Langevin, B.E. Mahi, M. Pinoche, Facilitated extraction and facilitated transport of non-ionic permeants through ion-exchange membranes: influence of the stability of the permeant/carrier complexes, J. Membr. Sci. 61 (1991) 191.

[5] M. Métayer, M. Legras, O. Grigorchouk, V. Nikonenko, D. Langevin, M. Labbé, L. Lebrun, V. Shaposhnik, Facilitated transport of α-alanine and phenylalanine through sulfonic cation-exchange membranes, Desalination 147 (2002) 375.

[6] J.A. Manzanares, R.M. Allen, K. Kontturi, Enhanced ion transfer rate due to the presence of zwitterionic phospholipid monolayers at the ITIES, J. Electroanal. Chem. 483 (2000) 188.

[7] V.A. Shaposhnik, T.V. Eliseeva, Barrier effect during the electrodialysis of ampholytes, J. Membr. Sci. 161 (1999) 223.

[8] T.V. Eliseeva, V.A. Shaposhnik, Effect of circulation and facilitated electromigration in electrodialysis with ion-exchange membranes, Russ. J. Electrochem. 36 (2000) 64.

[9] R. Simons, Electric field effects on proton transfer between ionizable groups and water in ion exchange membranes, Electrochim. Acta 29 (1984) 151.

[10] S.F. Timashev, E.V. Kirganova, Mechanism of the electrolytic decomposition of water molecules in bipolar ion-exchange membranes, Sov. Electrochem. 17 (1982) 366 (Elektrokhimiya 17 (1982) 440).

[11] V.V. Umnov, N.V. Sheldeshov, V.I. Zabolotskii, Current–voltage curve for the space charge region of a bipolar membrane, Russ. J. Electrochem. 35 (1999) 871.

[12] J.J. Krol, M. Wessling, H. Strathmann, Concentration polarization with monopolar ion exchange membranes: current–voltage curves and water dissociation, J. Membr. Sci. 162 (1999) 145.

[13] S. Mafé, P. Ramirez, A. Alcaraz, V. Aguilella, Ion transport and water splitting in bipolar membranes: theoretical background, in: A.J.B. Kemperman (Ed.), Handbook on Bipolar Membranes Technology, Twente University Press, Twente, 2000.

[14] A. El Attar, A. El Midaoui, N. Pismenskaia, C. Gavach, G. Pourcelly, Comparison of transport properties of monovalent anions through anion exchange membranes, J. Membr. Sci. 143 (1998) 249.

[15] N. Pismenskaya, E. Laktionov, V. Nikonenko, A. El Attar, B. Auclair, G. Pourcelly, Dependence of composition of anion-exchange membranes and their electrical conductivity on concen-

tration of sodium salts of carbonic and phosphoric acids, J. Membr. Sci. 181 (2000) 185.
[16] N. Pismenskaya, V. Nikonenko, E. Volodina, G. Pourcelly, Electrotransport of weak-acid anions through anion exchange membranes, Desalination 147 (2002) 345.
[17] T.V. Eliseeva, V.A. Shaposhnik, Transport of carbonates through an anion exchange membrane in electrodialysis, Russ. J. Electrochem. 36 (2000) 902.
[18] J.A. Manzanares, W.D. Murphy, S. Mafé, H. Reiss, Numerical simulation of the nonequilibrium diffuse double layer in ion-exchange membranes, J. Phys. Chem. 97 (1993) 8524.
[19] V.V. Nikonenko, V.I. Zabolotskii, K.A. Lebedev, Model for the competitive transport of ions through ion exchange membranes with a modified surface, Russ. J. Electrochem. 32 (1996) 234.
[20] V.V. Zabolotsky, V.I. Nikonenko, Ion Transport in Membranes (in Russian), Nauka, Moscow, 1996.
[21] F. Helfferich, Ion Exchange, McGraw-Hill, New York, 1962, p. 134.
[22] V.V. Nikonenko, M.Kh. Urtenov, On a generalization of the electroneutrality condition, Russ. J. Electrochem. 32 (1996) 195.
[23] M.K. Urtenov, V.V. Nikonenko, Analysis of the boundary-value problem solution of the Nernst–Planck–Poisson equations, 1:1 electrolytes, Russ. J. Electrochem. 29 (1993) 314.
[24] I. Rubinstein, B. Zaltzman, Electro-osmotically induced convection at a permselective membrane, Phys. Rev. E 62 (2) (2000) 2238 (Part A).
[25] M. Eigen, Proton transfer, acid–base catalysis, and enzymatic hydrolysis, Angew. Chem. Int. Ed. 3 (1964) 1.